

High-gain antenna arrays for millimetre-wave energy harvesting: architectures, challenges, and future directions

Shalini Mirle Gajendra, Naveen Kalenahalli Bhoganna

Department of Electronics and Communication Engineering, BGS Institute of Technology, Adichunchanagiri University, Bellur, India

Article Info

Article history:

Received Nov 19, 2025

Revised Feb 16, 2026

Accepted Apr 20, 2026

Keywords:

Artificial intelligence-driven adaptive beamforming
Battery-free internet of things devices
Beamforming techniques
High-gain antenna arrays
Metasurface-enhanced rectennas
mmWave energy harvesting

ABSTRACT

The rapid expansion of fifth-generation (5G)/sixth-generation (6G) networks and internet of things (IoT) ecosystems has intensified the need for self-sustaining power solutions to support billions of wireless devices. Millimetre-wave (mmWave) energy harvesting (EH) emerges as a viable alternative to traditional battery-powered systems, leveraging ambient radio frequency (RF) signals to provide continuous energy for IoT, smart sensor networks, and next-generation wireless applications. However, several challenges hinder its widespread adoption, including high path loss, low RF-to-direct current (DC) conversion efficiency, and the trade-off between high gain and wide bandwidth. This paper presents a comprehensive review of high-gain mmWave antenna arrays, exploring state-of-the-art advancements in beamforming techniques, phased arrays, metasurface-enhanced rectennas, and multi-band EH architectures. We analyse existing methodologies, identifying key research gaps such as scalability constraints, material limitations, and real-world deployment challenges. Additionally, we highlight emerging trends, including artificial intelligence (AI)-driven adaptive beamforming, intelligent metasurfaces, and cost-effective fabrication techniques, which can significantly improve mmWave RF EH efficiency. By addressing these gaps, this study provides insights into future research directions for developing high-performance, scalable, and commercially viable mmWave EH solutions. The findings pave the way for the practical deployment of battery-free IoT devices, smart city infrastructures, and energy-autonomous wireless communication networks in the 6G era.

This is an open access article under the [CC BY-SA](https://creativecommons.org/licenses/by-sa/4.0/) license.



Corresponding Author:

Shalini Mirle Gajendra

Department of Electronics and Communication Engineering, BGS Institute of Technology

Adichunchanagiri University

Bellur, India

Email: Shalini_180701@rediffmail.com

1. INTRODUCTION

Communication technologies are being revolutionised by fifth-generation (5G) and soon-to-be sixth-generation (6G) wireless networks, which offer extremely fast data rates, minimal latency, and extensive connectivity. Applications like the internet of things (IoT), augmented reality (AR), virtual reality (VR), smart cities, and driverless cars are all supported by these networks. IoT devices, in particular, are becoming an integral part of smart environments, healthcare, industrial automation, and smart agriculture [1]. However, a major challenge associated with the massive deployment of IoT devices is energy supply. Since IoT devices are often deployed in remote or inaccessible locations, relying on traditional battery-powered solutions introduces limitations due to frequent recharging, maintenance costs,

and environmental concerns. In order to create a self-sustaining power source for the IoT and wireless sensor networks (WSNs), this has prompted research into alternate energy sources, including wireless energy harvesting (EH) techniques [2], has been conducted. Radio frequency (RF) EH has become a promising technology among energy-harvesting options, allowing devices to absorb and transform ambient electromagnetic (EM) waves into electrical energy that may be used [3]. This makes it the perfect option for wireless and self-sufficient networks since it does not require wired power sources or frequent battery replacements.

Traditional energy-harvesting methods, such as solar, vibration, and thermoelectric energy, have been explored for powering IoT and WSNs. However, these methods often suffer from intermittent energy availability, depending on environmental conditions [4]. RFEH, on the other hand, offers a continuous and omnipresent source of energy by capturing EM signals from various sources, such as Wi-Fi, cellular networks, satellite transmissions, and dedicated RF power beacons [5]. Advantages of RFEH over other energy sources. Availability: unlike solar or thermoelectric energy, which depends on external factors, RF energy is continuously available in urban areas with high wireless traffic. Scalability: RFEH can be integrated into a wide range of devices, from implantable medical sensors to autonomous drones and large-scale IoT networks. Compatibility with wireless networks: as IoT networks continue expanding, RFEH can seamlessly co-exist with 5G and 6G networks, utilising their transmissions for simultaneous EH and communication. However, one of the biggest limitations of RFEH is low power density.

Since ambient RF power is often weak (typically in the μW to mW range), efficient antenna design and high-gain energy capture techniques are required to make it a viable power source. While traditional RFEH has focused on sub-6 GHz frequencies (e.g., Wi-Fi at 2.4 GHz, cellular networks at 900 MHz, and 1,800 MHz), recent research has shifted towards millimetre-wave (mmWave) EH (24-100 GHz) due to the following advantages: compact antenna size: at mmWave frequencies, the wavelength is significantly smaller, allowing for compact and highly efficient antennas [6]. This enables seamless integration into IoT devices, wearables, and implantable biomedical sensors. Compared to traditional sub-6 GHz rectennas, mmWave rectennas can be designed with a much smaller form factor without compromising performance. Large spectral resources: the mmWave spectrum offers abundant bandwidth compared to the congested sub-6 GHz bands [7]. This allows for multi-frequency EH, improving overall energy conversion efficiency. Higher energy density: since power is proportional to frequency, mmWave signals inherently carry more energy per unit area, making them more effective for RFEH applications.

Despite these advantages, mmWave EH introduces several technical challenges that must be addressed. High free-space path loss mmWave signals experience greater path loss compared to sub-6 GHz frequencies, which means that high-gain antenna arrays are essential to compensate for signal degradation. Studies suggest that beamforming and phased array configurations are necessary for effective EH at mmWave frequencies. Directional nature of mmWave signals, unlike sub-6 GHz waves that propagate omnidirectionally, mmWave signals require precise beam alignment to ensure maximum energy absorption [8]. This necessitates the use of adaptive beamforming and phased array antennas for efficient mmWave RFEH. Material constraints and fabrication challenges, at higher frequencies, dielectric losses increase, reducing overall antenna efficiency. The choice of low-loss materials such as Rogers RT/duroid, liquid crystal polymer (LCP), and low-temperature co-fired ceramics (LTCC) is crucial for effective mmWave rectenna design.

Motivations and contributions of research work with the rapid evolution of 5G/6G networks and IoT ecosystems, the demand for self-sustaining wireless power solutions has surged. mmWave EH offers a promising alternative to traditional battery-dependent systems, enabling continuous power supply for IoT devices, sensors, and smart communication networks [9]. However, challenges such as high path loss, low RF-to-direct current (DC) conversion efficiency, and the trade-off between high gain and wideband operation hinder the widespread adoption of mmWave rectenna systems.

This study aims to bridge these gaps by exploring high-gain antenna arrays, adaptive beamforming techniques, and multi-band EH solutions for efficient and scalable mmWave EH systems. Further contributions of research work are as follows: comprehensive survey on high-gain mmWave antennas—analyses existing antenna architectures, phased arrays, metasurface designs, and reconfigurable intelligent surface (RIS)-assisted systems for optimising power collection efficiency. Evaluation of beamforming and multi-frequency rectenna systems—reviews adaptive phase shifters (APS), AI-driven optimisation, and hybrid rectenna networks to enhance RF-to-DC conversion in dynamic environments. Identification of key research gaps in mmWave EH—highlights gain-bandwidth trade-offs, scalability challenges, material constraints, and integration barriers affecting real-world deployment. Future research directions for large-scale deployment—proposes AI-assisted beamforming, intelligent metasurfaces, and cost-effective fabrication techniques to accelerate the adoption of self-powered IoT and 6G networks.

2. RELATED WORK

In recent years, significant advancements have been made in the field of mmWave EH and high-gain antenna array design, focusing on improving efficiency, reducing hardware complexity, and optimizing beamforming strategies. Various studies have explored different techniques to address the key challenges associated with mmWave networks. These challenges include path loss, directional energy reception, and integration with intelligent surfaces.

2.1. Millimetre-wave

Investigates the role of RIS in mmWave EH to enhance energy coverage and efficiency [10]. By formulating an analytical framework based on stochastic geometry, the study derives a closed-form expression for energy coverage probability (ECP) and proposes an analytical model for average harvested energy (AHE). The results demonstrate that RIS-assisted mmWave networks can significantly improve EH performance, particularly in urban environments where high path loss is a major constraint. To further improve beamforming efficiency and minimise hardware complexity, APS have been introduced for hybrid beamforming techniques. In [11] presents a novel APS hybrid beamforming scheme that reduces the dependency on the number of antenna arrays and RF chains. The proposed hybrid design achieves performance comparable to the fully connected iterative hybrid beamforming approach while significantly reducing the number of required phase shifters (PSs). A flexible deployment strategy is proposed, where the number of PSs can be adjusted dynamically, ranging from two per RF chain to a full-network configuration. Furthermore, the study employs a modified K-means algorithm to optimize PS utilization, thereby enhancing the overall efficiency of hybrid beamforming systems. In addition to beamforming advancements, antenna array configurations play a crucial role in enhancing gain and bandwidth efficiency. In [12] suggests a sub-array design that has four radiating slots that are connected to an E-plane groove gap waveguide via a rectangular coupling slot after being driven by a groove gap cavity. The research presents a corporate-fed distribution network that combines E-plane groove gap waveguide and ridge gap waveguide structures to provide a wideband, low-loss antenna array. A waveguide rectangular 6 (WR6) waveguide flange is integrated at the bottom of the array's 16×16 radiating slots to provide effective excitation. Similarly, by presenting a unique phase correction technique for transmitarrays, in [13] concentrates on gain increase in dual-polarised multibeam antenna arrays. In this work, two Butler matrices based on substrate-integrated waveguide (SIW) technology are vertically stacked to feed a 2×2 dual-polarised magneto-electric (ME) dipole antenna array in a three-layer printed circuit board (PCB) laminate construction. The dual-polarised 2D multibeam antenna achieves improved beamforming efficiency by using this novel phase correction technique, which makes it a viable option for wireless power transmission and next-generation mmWave EH applications.

Proposes a dual-circularly polarised (dual-CP) mmWave array antenna using a gap waveguide-based feeding structure [14]. The design incorporates a septum polariser and a turnstile orthomode transducer (OMT) to achieve dual-circular polarisation, where $\pm 90^\circ$ phase differences are introduced between the transverse electric (TE)₁₀ and TE₀₁ modes. The turnstile OMT enables the separation of these orthogonal modes into four mutually orthogonal subarrays, ensuring effective polarisation diversity and improved signal integrity. This dual-CP approach is particularly beneficial for mmWave EH systems, where polarisation flexibility enhances signal reception and conversion efficiency. To further enhance gain and efficiency, in [15] introduces a planar segmented patch antenna (PSA), which achieves a 3 dB gain enhancement compared to conventional patch antennas without requiring a superstrate stack-up layer. The PSA configuration leverages multiple segmented conductors to induce magnetic currents, generating a strong magnetic field circulation around the conductors. Unlike traditional patch antennas, this design requires only a single excitation port while shorting pins synchronise resonance currents across the segmented conductors, ensuring stable and efficient radiation performance. This approach enhances gain without significantly increasing the antenna's footprint, making it suitable for compact and high-performance mmWave EH systems. Another key development in high-gain mmWave antennas is the dual-polarized 8×8 antenna array, as proposed in [16]. This antenna system, designed for Q-band mmWave applications, incorporates metallic pillars and cavities acting as magnetoelectric dipoles. The design features a 1-to-4 backed cavity feeding mechanism with cross-shaped slots that effectively excite two orthogonal linear polarisations. The integration of shared via-based feeding networks enhances the antenna's bandwidth and polarisation stability. The fabricated prototype demonstrates high gain and broad bandwidth, reinforcing its potential for high-efficiency EH and power transfer applications in mmWave frequencies.

These studies highlight the diverse approaches to mmWave antenna design, focusing on dual-polarised configurations, segmented patch antennas, and magnetoelectric dipole-based arrays. By integrating these innovative techniques, future mmWave EH systems can achieve higher efficiency, better polarization control, and improved compactness, facilitating their deployment in next-generation wireless

energy networks and IoT applications. In [17] introduces a novel broadband, multibeam ambient mmWave EH device with high yield. To address the issues of battery replacement and charging in industrial IoT applications, the suggested architecture combines a dual-polarised ME dipole rectenna array, a modified Luneburg lens, and a basic DC combiner. The system maximises EH from various angles and frequency bands by utilising diversity in frequency, space, and polarisation. By enabling RF signal combining and multibeam capabilities, the improved Luneburg lens greatly increases power-gathering efficiency. Additionally, a simplified rectifier network is incorporated to enhance RF-to-DC conversion, ensuring a more effective and stable energy output for IoT-based mmWave-powered applications. Hybrid strategies that combine sub-6 GHz and mmWave networks provide more EH options than stand-alone mmWave systems. In [18] investigates a hybrid network deployment in which mmWave or sub-6 GHz base stations (BSs) may both provide information and energy to user equipment (UE) at the same time. The study offers analytical models for ECP and signal-to-interference-plus-noise coverage probability (SCP) using a stochastic geometry framework. A detailed description of EH performance under various network situations is made possible by the suggested framework, which uses poisson point processes (PPP) and poisson cluster processes (PCP) to represent the locations of BS and UE. Both studies underscore the advancements in mmWave-based EH, with one focusing on high-gain rectenna and multibeam techniques and the other on hybrid network deployments combining sub-6 GHz and mmWave sources. These approaches pave the way for scalable, multi-source EH systems, addressing challenges such as beam misalignment, variable signal availability, and energy conversion efficiency in next-generation wireless networks. Table 1 shows the summary of recent advances in mmWave EH and antenna design.

Table 1. Summary of recent advances in mmWave EH and antenna design

Reference	Methodology	Advantages	Shortcomings
[10]	Utilisation of RIS in mmWave networks to enhance EH through stochastic geometry modelling.	Improves ECP and harvested energy efficiency in urban environments with high path loss.	The study is theoretical and lacks experimental validation or real-world deployment results.
[11]	Introduction of APS for hybrid beamforming to reduce hardware complexity while maintaining high performance.	Achieves performance comparable to fully connected hybrid beamforming but with fewer PSs, optimising power and computational efficiency.	Practical implementation challenges and the impact of APS variations on real-world network performance are not explored.
[12]	Creation of an E-plane groove gap waveguide and ridge gap waveguide for a corporate-fed sub-array arrangement.	Achieves wideband and low-loss performance with efficient energy transfer through a 16×16 radiating slot configuration.	Fabrication complexity and integration challenges in real-world scenarios are not addressed.
[13]	Proposal of a novel phase compensation method for transmitarray-based dual-polarised multibeam antenna design.	Enhances gain efficiency in dual-polarised antennas using a three-layer PCB laminate with SIW-based Butler matrices.	Limited discussion on the impact of environmental factors and real-world deployment feasibility.
[14]	design of a gap waveguide-based dual-CP millimetre wave array antenna.	Provides enhanced polarisation flexibility and improved signal reception for EH applications.	Requires complex manufacturing processes and precise alignment for optimal performance.
[15]	Development of a PSA for improved gain efficiency.	reduces complexity by achieving a 3 dB gain improvement without the need for a superstrate stack-up layer.	Lack of real-world testing to validate its EH efficiency in practical environments.
[16]	An 8×8 dual-polarised antenna array with a wide bandwidth and good gain is proposed for use in Q-band millimetre wave applications.	Ensures improved EH efficiency through magnetoelectric dipole design and optimised feed structure.	Limited scalability analysis for large-scale deployment.
[17]	Installation of a ME-dipole rectenna array and a modified Luneburg lens to create a high-gain, multibeam mmWave EH system.	Enhances RF-to-DC conversion efficiency by leveraging frequency, spatial, and polarisation diversity.	Experimental results are needed to validate performance across different operating conditions.
[18]	Hybrid deployment of mmWave and sub-6 GHz networks for EH and information transfer at the same time.	Provides a flexible EH solution across multiple frequency bands and diverse network conditions.	The stochastic modelling approach lacks real-world validation and hardware implementation.

2.2. Antenna array configurations and optimisation techniques

The difficulties in obtaining a broad axial ratio and impedance bandwidth overlap in patch antenna arrays have been brought to light by recent investigations. According to [19], it is still challenging to achieve an overlapping bandwidth of 20% even when L-type probe feeding and sequential rotation (SR) approaches are used. Yang *et al.* [20] addressed the issue by extending the axial ratio bandwidth to about 30% using a dielectric resonator antenna (DRA) method. However, DRAs are less feasible for large-scale mmWave applications due to their complexity and high manufacturing costs. Similar to this, a 3D helical structure was

employed in [21] to attain a 20% 3-dB axial ratio bandwidth; however, putting such a structure together for mmWave applications is extremely difficult. Furthermore, it is expensive to fabricate using the LTCC method. Another method for transforming linearly polarised (LP) beams into circularly polarised (CP) beams was investigated in [22] using a circular polariser. Although efficient, this approach lengthens the antenna's longitudinal length and adds extra losses, which makes it less appropriate for small designs. ME dipole antennas have drawn a lot of interest among wideband radiating elements because of their superior polarisation and impedance matching capabilities. For example, an aperture-coupled ME-dipole antenna created in [23] had a 3-dB AR bandwidth of 17.3% and an impedance bandwidth of 24.9%. ME-dipole antennas have included SR techniques to increase CP radiation and expand the axial ratio bandwidth. Using the SR approach, Feng *et al.* [24] created a 4×4 ME-dipole antenna fed by a SIW, achieving a 3-dB axial ratio bandwidth of 27.8% and an impedance bandwidth of 27.7%. However, at mmWave frequencies, SR-feed network integration is challenging due to the rigidity of SIW structures, which restricts antenna design flexibility.

The complementary source technique has been shown to be a more effective way to enhance CP radiation in mmWave antenna arrays than the SR technique. An aperture-coupled complementary antenna was proposed by Ji *et al.* [25], and it achieved a 3-dB axial ratio bandwidth of 38.8% (from 53.57 to 79.32 GHz) and a broad impedance bandwidth of 33.8% (from 56.11 to 78.95 GHz). According to these findings, complementary source approaches present a viable substitute for attaining high-performance CP radiation in mmWave antenna arrays while preserving a larger bandwidth. With a peak gain of 13 dBi and 80° angular coverage, the system presented in [26] uses a Rotman lens-based design for 5G mmWave EH and runs at 28 GHz. When running at an input power of 10 dBm, its overall efficiency is still low at 10%, indicating a number of issues that must be fixed for better performance. The use of traditional microstrip patch antennas, which by their very nature have a limited bandwidth, is a significant disadvantage of this Rotman lens-based technology. Furthermore, the design becomes more complex as the number of Rotman lens ports rises, which results in a decline in performance due to metallic losses. The system in [26] is restricted to an eight-port Rotman lens arrangement to offset these losses, which limits the potential gain and renders it unsatisfactory for mmWave EH applications. The limited beam deflection coverage is yet another significant drawback.

Although [27] tried to increase the coverage angle to 110° by adopting a flexible PCB design, the Rotman lens's flexibility for a variety of EH scenarios is limited because it can only deflect beams in one dimension. Additionally, the Rotman lens's direct connection of several ports enhances mutual coupling effects, requiring the inclusion of high-frequency capacitors to inhibit DC feedback. This raises the system's cost considerably. Additional improvement is also needed for the DC combining circuit utilised in the multiport EH systems of today. N is the number of rectifier diodes, and even though [27] offered an efficient short-circuit diode network that builds upon the models from [28] and [29], the design still requires $2 \times (N-1)$ bypass diodes. Scalability is a major challenge because this method becomes unfeasible as the number of ports rises. A high-gain, multidimensional, large-angle beam scanning system that is more appropriate for mmWave EH must be the main focus of a reevaluation of the EH architecture in light of these limitations. To increase efficiency and scalability, future designs should investigate reduced mutual coupling techniques, alternate beamforming procedures, and affordable high-frequency rectification techniques. An overview of antenna array layouts and optimisation methods is provided in Table 2.

Work introduces a fresh multiple-input multiple-output (MIMO) antenna array featuring eight compact trapezoidal slot elements and L-shaped coplanar waveguide (CPW) feedlines, tailored for sub-6 GHz 5G needs. This setup delivers wide bandwidth and polarisation diversity, supporting solid links in the 3.2-6 GHz band. Positioned at smartphone corners, the antennas fit a compact 75 mm by 150 mm space, and achieve strong isolation sans decoupling structures. The array boasts 2,800 MHz bandwidth, low envelope correlation coefficient (ECC) < 0.005 , and total active reflection coefficient (TARC) < -20 dB for top radiation efficiency. Built affordably on a single-layer flame retardant level 4 (FR4) substrate, tests match simulations closely. It also proposes a compact mmWave phased array to enable high data rates, better connectivity, and easy smartphone use for future 5G/6G. Meanwhile, deeply analyses near-field impulse responses in a double-slot Vivaldi antenna, extending past MIMO systems. It uses EM near-field data to track EM energy flow, reorientation, and scattering over antenna parts. By studying near-field wavefront surfaces' shapes, the work evaluates structural tweaks and antenna directivity. To clarify EM propagation in Vivaldi antennas, it streamlines the near-field propagation model with partitioned far-field response traits in frequency and time domains.

This approach pinpoints key EM flow spots and gauges how structures affect radiation performance, steering future designs. Validation draws on near-field, far-field, and standard radiation traits, proving its fit for other travelling-wave antennas to fine-tune performance and study propagation. Study describes a wideband dual-polarized dipole antenna working from 1.7 to 3.8 GHz, marking a key step forward in

sub-6 GHz antenna tech. Classic 4G dipole antennas often struggle with impedance matching and radiation pattern stability, particularly for 5G sub-6 GHz use. To overcome this, the design adds a connected-ring-shaped metasurface structure acting as an artificial magnetic conductor (AMC). This AMC setup steadily holds radiation patterns without increasing antenna height, aiding real-world use in next-gen BSs. Tests verify an 80.7% impedance bandwidth (1.7-4.0 GHz), steady half-power beamwidth (HPBW) of $70^{\circ} \pm 5^{\circ}$, and realised gain of 7.0 ± 1.0 dBi. Its straightforward build ensures it fits seamlessly with 4G and 5G networks, boosting potential for BS setups.

Table 2. overview of antenna array configurations and optimisation techniques

Reference	Methodology	Advantages	Shortcomings
[19]	Investigates axial ratio and impedance bandwidth overlap in patch antenna arrays. Uses L-type probe and SR feeding.	Provides a method to improve axial ratio bandwidth in patch antennas.	Fails to achieve a 20% overlapping bandwidth even with SR feeds.
[20]	Implements DRA techniques to expand AR bandwidth to 30%.	Achieves a broader axial ratio bandwidth compared to conventional patch antennas.	DRA technology is complex and costly, limiting scalability.
[21]	Utilises a 3D helical structure to achieve a 20% 3-dB axial ratio bandwidth.	Provides stable CP radiation characteristics.	Complex 3D assembly makes it difficult to implement at mmWave frequencies.
[22]	Proposes a circular polariser to convert LP beams into CP beams.	Enhances CP radiation without modifying the antenna structure.	Introduces additional loss and increases the antenna's longitudinal size.
[23]	Develops an aperture-coupled ME dipole antenna achieving a 24.9% impedance bandwidth and 17.3% 3-dB axial ratio bandwidth.	Achieves wideband CP radiation with improved impedance matching.	Limited flexibility in design adjustments for further bandwidth enhancement.
[24]	Designs a 4×4 SIW-fed ME-dipole antenna using an SR technique to enhance CP performance.	Achieves 27.7% impedance bandwidth and 27.8% axial ratio bandwidth, improving CP stability.	SIW structures have limited flexibility, making implementation difficult at mmWave frequencies.
[25]	Proposes an aperture-coupled complementary antenna achieving CP radiation at mmWave frequencies.	Achieves an impedance bandwidth of 33.8% and a 3-dB axial ratio bandwidth of 38.8%.	Implementation and fabrication complexity at high frequencies.
[26]	Develops a Rotman lens-based mmWave EH system operating at 28 GHz.	Provides 80° angular coverage for 5G mmWave EH.	Low efficiency (10% at 10 dBm input), design complexity, and high mutual coupling.
[27]	Extends Rotman lens coverage angle to 110° using a flexible PCB design.	Enhances angular coverage and flexibility.	Beam deflection is still limited to one dimension, requiring high-frequency capacitors to block DC feedback.
[28]	Optimizes a short-circuit diode network for EH rectifier circuits.	Reduces losses in rectification processes.	Requires $2 \times (N-1)$ bypass diodes, making large-scale implementations impractical.
[29]	Further refines rectifier circuit design for Rotman lens-based RF EH.	Improves rectification efficiency.	Scalability issues remain due to component complexity.

Discusses the drawbacks of conventional array antenna reliability assessment techniques, particularly those that rely on the n/k system and have a tendency to exaggerate reliability by ignoring the impact of malfunctioning transmit/receive (T/R) modules [30]. A novel reliability evaluation method that takes into account performance variations brought on by T/R failures at various array locations is suggested in order to increase accuracy. By examining every possible condition of the antenna system, this approach guarantees a more accurate dependability evaluation. The system is separated into subarrays for large-scale antenna arrays, and each subarray is assessed separately. The study improves the overall fault tolerance model by introducing a minimum failure threshold for every subarray. According to simulation results, this method provides a more realistic reliability assessment for high-density antenna deployments by lowering overestimation errors. This approach is especially helpful for phased array and huge MIMO systems, where smooth operation depends on excellent dependability. In [31] offers the design of a zero-order resonant antenna based on the composite right-left-handed (CRLH) concept, operating at 30 GHz, to further improve performance in small mmWave applications.

The antenna uses mirror-image CRLH structures for patch-like radiation and is constructed without metallic vias. Dispersion diagrams, parameter extraction, and similar circuit modelling are used to examine its performance. With an 87% radiation efficiency and a realised gain of 5.35 dBi, the experimental prototype ensures efficient energy use. With a 10 GHz bandwidth and no spurious resonance, the design exhibits reliable performance for high-frequency applications. Furthermore, a 4×4 Butler matrix is used to create a passive beamforming array that connects CRLH antennas to provide beam-scanning angles of 12°, -68°, 64°,

and -11° . As a small, highly effective solution for next-generation wireless networks, the results validate the antenna's applicability for 5G, wireless power transfer, and IoT sensing applications. In addition to traditional resonant antennas, in [32] presents a new graphene-based antenna that has four graphene sheet reflectors and a dipole. It can adjust its beam dynamically by tuning its chemical potentials with an electric field. This allows for 360° azimuthal beam steering and quasi-omnidirectional, one-directional, or two-directional beam combinations. To further increase the antenna's versatility, a second graphene layer is incorporated to regulate radiation patterns in the elevation plane. Depending on the activation regime, the antenna's variable gain ranges from 0.86 to 1.63 dBi when operating in the 1.75-2.03 THz frequency band. Radiation properties are predicted using a group-theoretical analytic approach, which lowers computational complexity and increases design efficiency. The proposed graphene antenna facilitates real-time beam control, making it well-suited for THz communication, tracking moving transmitters, medical imaging, and security screening applications. The antenna's theoretical performance is validated by numerical simulations, and further study will concentrate on increasing radiation efficiency and expanding its possible uses.

Research looks at how common-mode (CM) currents create interference between low-band (690-960 MHz) and high-band (1,810-2,690 MHz) antenna elements, leading to pattern distortion in multiband base-station antennas. To fix this, the high-band impedance matching network adds a special CM suppression circuit that shifts the CM resonance frequency away from the low-band area. This modification greatly enhances low-band radiation patterns and minimises undesired distortions. The suppression method reduces intercell interference, improves network performance, and guarantees stable beamwidth variation ($65^\circ \pm 5^\circ$) for low-band transmissions, according to experimental validation. High-band performance and appropriate impedance matching are maintained while CM currents are efficiently suppressed using a quarter-wavelength short line with a capacitor. This method is ideal for next-generation 5G BSs because it maximises multiband antenna efficiency. A new ultra-wideband (UWB) antenna with a straightforward yet efficient design is presented by [33] in response to the increasing need for small, flexible, and wideband antennas. The antenna incorporates a semi-circular stub and triangular slots into a traditional rectangular monopole design. It is made of a flexible Rogers 5880 substrate with low dielectric loss and a narrow profile (0.254 mm). The impedance bandwidth is greatly increased by these changes, spanning a broad frequency range of 2.73-9.68 GHz.

The antenna's small 15×20 mm² form factor makes it ideal for wearable technology and flexible electronics. Performance tests verify that the antenna's mechanical resilience and flexibility are maintained even when bent along the x and y axes, resulting in steady radiation characteristics. It is a great option for small wireless communication systems since it produces an omnidirectional radiation pattern with a minimum gain greater than 2.5 dBi. Furthermore, the CPW feeding approach makes it easier to integrate with electrical circuits, which increases its usefulness in applications for flexible devices and the next generation of the IoT. In addition to physical antenna designs, in [34] introduces two computational methods for near-field modelling of spatially fed planar array antennas. One model relies on the A and F vector potentials to create radiation equations. The other builds on a superposition of far-field contributions from separate array members. These approaches show strong alignment, with relative error under 3.2% at 13λ , despite different core assumptions. Next, the faster model helps refine near-field beam-shaping for 5G mmWave setups. It optimises reflectarray layouts at 28 GHz via phase-only synthesis (POS), then applies the method of moments based on local periodicity (MoM-LP) for multi-frequency tweaks. This delivers a magnitude ripple under 1.5 dB and meets 5G new radio (NR) n257 band standards. The outcomes confirm that wideband near-field beam shaping suits spatially fed array antennas, offering a solid choice for beamforming and efficient mmWave indoor networks.

A design proposes a 5G mmWave glass antenna printed directly onto thick car windows, eliminating the need for structural changes or add-on parts. The antenna incorporates CPW, printed monopole, parasitic elements, a linearly arranged patch director, and a grid-slotted patch reflector. These director and reflector components boost bore-sight gain to support strong performance in vehicle mmWave communication. Tests show a reflection coefficient of -33.1 dB and peak gain of 6.2 dBi at 28 GHz, confirming reliable broadband operation across 24.1 GHz to 31.0 GHz. Real-world building and testing match the models closely, proving the antenna holds steady even on larger glass windows. It delivers a consistent bore-sight gain of 4.5 dBi, making it well-suited for 5G-enabled smart cars. Beyond cars, RF EH plays a key role in powering self-reliant IoT and 5G devices. Research explores its use to supply wireless networks and IoT setups, particularly for Industry 4.0 needs. It stresses creating systems that run without upkeep, save energy, and cut reliance on cables or batteries. Key focuses include better efficiency, circular polarisation, and smaller sizes, alongside handling rectifier nonlinearity's impact on energy conversion. The work reviews antenna configurations, impedance-matching networks, and rectifier designs, with special attention to biomedical and IoT uses. Table 3 outlines advanced antenna designs and ways to optimise them.

Table 3. Summary of advanced antenna designs and optimisation techniques

Reference	Methodology	Advantages	Shortcomings
[35]	Designs a sub-6 GHz MIMO antenna array with eight trapezoidal slot elements and L-shaped CPW feedlines.	Achieves wide bandwidth, high isolation, and polarisation diversity, optimised for smartphone integration.	Limited to sub-6 GHz frequencies, requiring further adaptation for mmWave applications.
[36]	Analyses near-field impulse responses in a double-slot Vivaldi antenna using EM near-field data.	Provides detailed insights into EM energy flow, optimising antenna directivity and structural performance.	The complexity of near-field modelling may limit practical implementation in large-scale networks.
[37]	Develops a wideband dual-polarised dipole antenna with a metasurface-based AMC.	Stabilises radiation patterns without increasing antenna height, achieving 80.7% impedance bandwidth.	Limited discussion on performance in highly dense urban environments with multipath effects.
[30]	Evaluates array antenna reliability by considering T/R module failures and subarray division.	Improves reliability assessment for massive MIMO and phased array systems.	Does not address hardware-level solutions for mitigating failures in real-time applications.
[31]	Designs a zero-order resonant antenna at 30 GHz using CRLH structures, analysed through equivalent circuit modelling.	Offers high efficiency (87%) with stable 10 GHz bandwidth and beam-scanning capabilities.	Gain remains moderate (5.35 dBi), limiting its application in high-power transmission scenarios.
[32]	Develop a graphene-based THz antenna with tunable beam control via electric field tuning.	Enables 360° beam steering with dynamic radiation pattern control, ideal for THz applications.	Low gain (0.86-1.63 dBi) reduces efficiency, requiring further improvements for long-range communication.
[38]	Proposes a CM suppression circuit to mitigate interference in multiband base-station antennas.	Improves network performance by minimising CM distortions and enhancing low-band stability.	Focuses on sub-6 GHz frequencies, requiring adaptations for mmWave and higher-frequency networks.
[33]	Designs an UW flexible antenna with a CPW-fed structure on Rogers 5880 substrate.	Maintains stable radiation even when bent, ensuring flexibility and robustness for wearable devices.	A lower gain (>2.5 dBi) may not be sufficient for long-range wireless applications.
[34]	Develops near-field models for spatially fed planar arrays, applying POS for beam shaping.	Achieves compliance with 5G NR n257 band, optimising beamforming for indoor mmWave networks.	Model complexity may hinder real-time adaptability in highly dynamic environments.
[39]	Proposes a glass-integrated 5G mmWave antenna for vehicular applications.	Provides broadband operation (24.1-31.0 GHz) without requiring vehicle modifications.	Bore-sight gain (6.2 dBi) remains moderate, limiting long-range communication potential.
[40]	Reviews RF EH for IoT and 5G networks, highlighting rectifier efficiency and miniaturisation challenges.	Identifies key advancements in impedance matching, rectification, and self-powered IoT systems.	Lacks experimental validation of proposed techniques in large-scale deployments.

Introduces a beamforming tri-band harvester designed to capture RF energy from GSM-900, DCS-1800, and Wi-Fi-2400 frequency bands [41]. The system integrates a novel tri-band Butler matrix with asymmetric hybrid couplers, functioning as the beamforming network to optimise spatial coverage while maintaining high-gain EH. Additionally, the study proposes a tri-band rectifying circuit featuring a single-branch impedance matching network, ensuring efficient RF-to-DC conversion at all three frequency bands. This approach enables multi-frequency EH, making it particularly valuable for IoT and smart WSNs that operate across diverse frequency ranges. To further enhance RFEH efficiency, in [42] presents a high-gain RFEH circuit that incorporates a 2×2 patch array antenna, a reflector, and a cascade microstrip L-matching network. The L-matching network serves as a passive voltage amplifier, boosting the induced voltage across the antenna to improve overall harvesting performance. The RFEH receiver is fabricated on a cost-effective FR-4 substrate, featuring a dielectric constant of 4.6 and a copper thickness of 0.035 mm. To further enhance RF-to-DC conversion efficiency, a novel microstrip voltage amplifier is integrated into the rectifier circuit, achieving a total gain of 30 dB at an input power of -30 dBm with a 1-MΩ load. This approach ensures higher power conversion efficiency, making it an ideal candidate for low-power wireless applications such as remote sensing, battery-free IoT nodes, and energy-autonomous communication networks. Beyond multi-band and high-gain harvesting circuits, in researchers [43]–[46] introduces a low-profile rectenna with high gain and wide angular coverage, specifically designed for RFEH and wireless power transmission applications. The system features a compact travelling-wave antenna array with spatially multiplexed radiation patterns, ensuring optimised energy reception from multiple angles. To improve rectification efficiency, a miniature rectifying circuit is integrated with a DC power combiner, delivering stable DC output power despite variations in incident RF wave angles [47]–[50]. This design addresses the challenge of directional dependence in RFEH, enabling more efficient energy capture in dynamic environments such as smart cities, autonomous sensor networks, and wearable electronics.

2.3. Research gap

Gain vs. bandwidth trade-off high-gain antenna arrays typically suffer from narrow bandwidth, limiting multi-frequency harvesting capability. Need for hybrid resonant structures, metasurfaces, or fractal designs to achieve simultaneous high gain (≥ 30 dBi) and wide bandwidth ($\geq 20\%$). Beamforming efficiency for EH. Most beamforming techniques focus on communication rather than energy collection. Research is needed in adaptive beamforming that dynamically aligns with high-power RF sources for maximum EH. Material and fabrication challenges conventional SIW, LTCC, and graphene-based antennas are costly and difficult to scale. Need for low-cost, flexible, and scalable substrates to enable mass production and real-world deployment. Scalability of large-scale mmWave EH networks. The implementation of multi-node RF harvesting grids remains underexplored. Future studies should focus on distributed EH architectures for large-scale 6G networks.

3. CONCLUSION

mmWave EH has emerged as a promising solution to address the growing demand for self-sustaining wireless power in 5G/6G networks, IoT ecosystems, and smart sensor applications. This study comprehensively reviews high-gain antenna arrays, beamforming techniques, and multi-frequency rectenna architectures, highlighting their role in optimising RF-to-DC conversion efficiency. Despite significant advancements, key challenges such as gain-bandwidth trade-offs, material constraints, scalability issues, and real-world deployment limitations remain unresolved. To bridge these gaps, future research must focus on AI-driven adaptive beamforming, intelligent metasurface-assisted rectennas, hybrid multi-band harvesting architectures, and cost-effective fabrication techniques. Additionally, large-scale experimental validation and integration with existing wireless networks are essential for practical implementation. Addressing these challenges will enable the widespread adoption of efficient, scalable, and high-performance mmWave EH solutions, paving the way for battery-free IoT devices, smart cities, and next-generation wireless communication systems.

ACKNOWLEDGEMENT

The authors gratefully acknowledge all who supported this research, especially our guide for his continuous guidance, insights, and encouragement.

FUNDING INFORMATION

No funding is raised for this research.

AUTHOR CONTRIBUTIONS STATEMENT

This journal uses the Contributor Roles Taxonomy (CRediT) to recognize individual author contributions, reduce authorship disputes, and facilitate collaboration.

Name of Author	C	M	So	Va	Fo	I	R	D	O	E	Vi	Su	P	Fu
Shalini Mirle Gajendra	✓	✓	✓		✓	✓		✓	✓	✓	✓			✓
Naveen Kalenahalli	✓	✓		✓	✓	✓		✓	✓	✓	✓	✓		
Bhoganna														

C : **C**onceptualization

M : **M**ethodology

So : **S**oftware

Va : **V**alidation

Fo : **F**ormal analysis

I : **I**nvestigation

R : **R**esources

D : **D**ata Curation

O : Writing - **O**riginal Draft

E : Writing - Review & **E**ditng

Vi : **V**isualization

Su : **S**upervision

P : **P**roject administration

Fu : **F**unding acquisition

CONFLICT OF INTEREST STATEMENT

The Author declares no conflict of interest.

DATA AVAILABILITY

No dataset is utilised in this research.





REFERENCES

- [1] T. A. Khan, A. Alkhateeb, and R. W. Heath, "Millimeter wave energy harvesting," *IEEE Transactions on Wireless Communications*, vol. 15, no. 9, pp. 6048–6062, Sep. 2016, doi: 10.1109/TWC.2016.2577582.
- [2] J. Zhang, X. Ge, Q. Li, M. Guizani, and Y. Zhang, "5G millimeter-wave antenna array: design and challenges," *IEEE Wireless Communications*, vol. 24, no. 2, pp. 106–112, Apr. 2017, doi: 10.1109/MWC.2016.1400374RP.
- [3] H. J. Basherlou, N. O. Parchin, and C. H. See, "Antenna design and optimization for 5G, 6G, and IoT," *Sensors*, vol. 25, no. 5, Feb. 2025, doi: 10.3390/s25051494.
- [4] Y. Zhang, R. Huang, G. Wang, Z. H. Jiang, and W. Hong, "A low-cost polarization detection approach enabled by energy harvesting metasurface: concept, design, and experiment," *IEEE Transactions on Microwave Theory and Techniques*, vol. 72, no. 10, pp. 6174–6186, Oct. 2024, doi: 10.1109/TMTT.2024.3381981.
- [5] S. Z. Aslam, A. Wilcher, B. Chatterjee, Y. K. Yoon, D. P. Arnold, and S. Sinha, "Challenges and opportunities in D-band transmitter architectures and antenna design, integration, and scalability for 6G communications: a brief review," *IEEE Access*, vol. 13, pp. 33849–33873, 2025, doi: 10.1109/ACCESS.2025.3542771.
- [6] D. Surender, M. A. Halimi, T. Khan, F. A. Talukdar, Nasimuddin, and S. R. Rengarajan, "5G/millimeter-wave rectenna systems for radio-frequency energy harvesting/wireless power transmission applications: an overview," *IEEE Antennas and Propagation Magazine*, vol. 65, no. 3, pp. 57–76, Jun. 2023, doi: 10.1109/MAP.2022.3208794.
- [7] H. Zhang, S. Huang, C. Jiang, K. Long, V. C. M. Leung, and H. V. Poor, "Energy efficient user association and power allocation in millimeter-wave-based ultra dense networks with energy harvesting base stations," *IEEE Journal on Selected Areas in Communications*, vol. 35, no. 9, pp. 1936–1947, Sep. 2017, doi: 10.1109/JSAC.2017.2720898.
- [8] B. Xu, Y. Chen, J. R. Carrion, J. Loo, and A. Vinel, "Energy-aware power control in energy cooperation aided millimeter wave cellular networks with renewable energy resources," *IEEE Access*, vol. 5, pp. 432–442, 2017, doi: 10.1109/ACCESS.2016.2633723.
- [9] O. L. A. Lopez, H. Alves, R. D. Souza, S. M.-Sanchez, E. M. G. Fernandez, and M. L.-Aho, "Massive wireless energy transfer: enabling sustainable IoT toward 6G era," *IEEE Internet of Things Journal*, vol. 8, no. 11, pp. 8816–8835, Jun. 2021, doi: 10.1109/JIOT.2021.3050612.
- [10] M. M. Saleh, N. A. Muhammad, N. Seman, and N. I. A. Apandi, "Stochastic geometry analysis of reconfigurable intelligent surface-assisted millimeter-wave energy harvesting networks," *IEEE Access*, vol. 13, pp. 47375–47388, 2025, doi: 10.1109/ACCESS.2025.3547837.
- [11] M. Alouzi, H. Yanikomeroglu, and G. K. Kurt, "Adaptive phase shifters for hybrid beamforming in mmWave systems," *IEEE Transactions on Wireless Communications*, vol. 24, no. 2, pp. 1104–1116, Feb. 2025, doi: 10.1109/TWC.2024.3505202.
- [12] A. Farahbakhsh, D. Zarifi, and A. Uz Zaman, "D-band high-gain planer slot array antenna using gap waveguide technology," *IEEE Transactions on Antennas and Propagation*, vol. 73, no. 1, pp. 594–599, Jan. 2025, doi: 10.1109/TAP.2024.3481909.
- [13] Z. Xu, S. Xu, Y. Shen, S. Xue, and S. Hu, "Gain enhancement of dual-polarized 2-D multibeam antenna with transmitarray," *IEEE Transactions on Antennas and Propagation*, vol. 72, no. 10, pp. 7574–7583, Oct. 2024, doi: 10.1109/TAP.2024.3442293.
- [14] Z. Liu, X. Cheng, and Y. Yao, "A novel wideband dual-circularly polarized array antenna for millimeter-wave communication," *IEEE Antennas and Wireless Propagation Letters*, vol. 23, no. 10, pp. 3232–3236, Oct. 2024, doi: 10.1109/LAWP.2024.3432894.
- [15] J. Kim and H. L. Lee, "High gain planar segmented antenna for mmWave phased array applications," *IEEE Transactions on Antennas and Propagation*, vol. 70, no. 7, pp. 5918–5922, Jul. 2022, doi: 10.1109/TAP.2022.3142333.
- [16] W. Zhao, X. Li, Z. Qi, and H. Zhu, "Broadband and high-gain dual-polarized antenna array with shared vias feeding network for 5G applications," *IEEE Antennas and Wireless Propagation Letters*, vol. 20, no. 12, pp. 2377–2381, Dec. 2021, doi: 10.1109/LAWP.2021.3112565.
- [17] F. Deng and K. M. Luk, "A broadband high-gain multibeam ambient millimeter-wave energy-harvesting system," *IEEE Internet of Things Journal*, vol. 11, no. 3, pp. 4888–4898, Feb. 2024, doi: 10.1109/JIOT.2023.3301536.
- [18] N. A. Muhammad, N. Seman, N. I. A. Apandi, and Y. Li, "Energy harvesting in sub-6 GHz and millimeter wave hybrid networks," *IEEE Transactions on Vehicular Technology*, vol. 70, no. 5, pp. 4471–4484, 2021, doi: 10.1109/TVT.2021.3068956.
- [19] M. Li and K.-M. Luk, "Low-cost wideband microstrip antenna array for 60-GHz applications," *IEEE Transactions on Antennas and Propagation*, vol. 62, no. 6, pp. 3012–3018, Jun. 2014, doi: 10.1109/TAP.2014.2311994.
- [20] M.-D. Yang, Y.-M. Pan, Y.-X. Sun, and K.-W. Leung, "Wideband circularly polarized substrate-integrated embedded dielectric resonator antenna for millimeter-wave applications," *IEEE Transactions on Antennas and Propagation*, vol. 68, no. 2, pp. 1145–1150, Feb. 2020, doi: 10.1109/TAP.2019.2938629.
- [21] C. Liu, Y.-X. Guo, X. Bao, and S.-Q. Xiao, "60-GHz LTCC integrated circularly polarized helical antenna array," *IEEE Transactions on Antennas and Propagation*, vol. 60, no. 3, pp. 1329–1335, Mar. 2012, doi: 10.1109/TAP.2011.2180351.
- [22] Y. Li, Z. N. Chen, X. Qing, Z. Zhang, J. Xu, and Z. Feng, "Axial ratio bandwidth enhancement of 60-GHz substrate integrated waveguide-fed circularly polarized LTCC antenna array," *IEEE Transactions on Antennas and Propagation*, vol. 60, no. 10, pp. 4619–4626, Oct. 2012, doi: 10.1109/TAP.2012.2207343.
- [23] Z. Gan, Z.-H. Tu, Z.-M. Xie, Q.-X. Chu, and Y. Yao, "Compact wideband circularly polarized microstrip antenna array for 45 GHz application," *IEEE Transactions on Antennas and Propagation*, vol. 66, no. 11, pp. 6388–6392, Nov. 2018, doi: 10.1109/TAP.2018.2863243.
- [24] B. Feng, J. Lai, K. L. Chung, T.-Y. Chen, Y. Liu, and C.-Y.-D. Sim, "A compact wideband circularly polarized magneto-electric dipole antenna array for 5G millimeter-wave application," *IEEE Transactions on Antennas and Propagation*, vol. 68, no. 9, pp. 6838–6843, Sep. 2020, doi: 10.1109/TAP.2020.2980368.
- [25] Z. Ji, G.-H. Sun, and H. Wong, "A wideband circularly polarized complementary antenna for millimeter-wave applications," *IEEE Transactions on Antennas and Propagation*, vol. 70, no. 4, pp. 2392–2400, Apr. 2022, doi: 10.1109/TAP.2021.3083782.
- [26] A. Eid, J. Hester, and M. M. Tentzeris, "A scalable high-gain and large-beamwidth mm-wave harvesting approach for 5G-powered IoT," in *2019 IEEE MTT-S International Microwave Symposium (IMS)*, 2019, pp. 1309–1312, doi: 10.1109/MWSYM.2019.8700758.
- [27] A. Eid, J. G. D. Hester, and M. M. Tentzeris, "5G as a wireless power grid," *Scientific Reports*, vol. 11, no. 1, Jan. 2021, doi: 10.1038/s41598-020-79500-x.
- [28] U. Olgun, C.-C. Chen, and J. L. Volakis, "Investigation of rectenna array configurations for enhanced RF power harvesting," *IEEE Antennas and Wireless Propagation Letters*, vol. 10, pp. 262–265, 2011, doi: 10.1109/LAWP.2011.2136371.
- [29] A. N. Parks and J. R. Smith, "Active power summation for efficient multiband RF energy harvesting," in *2015 IEEE MTT-S International Microwave Symposium*, May 2015, pp. 1–4, doi: 10.1109/MWSYM.2015.7167129.
- [30] X. Huang, S. Zhu, and G. Liang, "Reliability evaluation method for array antenna considering performance changes," *Sensors*, vol. 24, no. 6, Mar. 2024, doi: 10.3390/s24061914.
- [31] M. P. Mohan, H. Cai, A. Alphones, and M. F. Karim, "mmWave zero order resonant antenna with patch-like radiation fed by a Butler matrix for passive beamforming," *Sensors*, vol. 23, no. 18, Sep. 2023, doi: 10.3390/s23187973.





- [32] V. Dmitriev, R. M. S. D. Oliveira, R. R. Paiva, and N. R. N. M. Rodrigues, "Multifunctional THz graphene antenna with 360° continuous ϕ -steering and θ -control of beam," *Sensors*, vol. 23, no. 15, Aug. 2023, doi: 10.3390/s23156900.
- [33] E. Ali *et al.*, "A shorted stub loaded UWB flexible antenna for small IoT devices," *Sensors*, vol. 23, no. 2, Jan. 2023, doi: 10.3390/s23020748.
- [34] D. R. Prado, "Near field models of spatially-fed planar arrays and their application to multi-frequency direct layout optimization for mm-Wave 5G new radio indoor network coverage," *Sensors*, vol. 22, no. 22, Nov. 2022, doi: 10.3390/s22228925.
- [35] H. J. Basherlou, N. O. Parchin, and C. H. See, "A dual-polarized and broadband multiple-antenna system for 5G cellular communications," *Sensors*, vol. 25, no. 4, Feb. 2025, doi: 10.3390/s25041032.
- [36] H. Hoang, M.-H. Nguyen, and V. P.-Xuan, "Analysis of near-field characteristics on improved structures of double-slot antipodal Vivaldi antenna," *Sensors*, vol. 24, no. 15, Aug. 2024, doi: 10.3390/s24154986.
- [37] X. Lin, J. Mai, H. He, and Y. Zhang, "Dual-polarized dipole antenna with wideband stable radiation patterns using artificial magnetic conductor reflector," *Sensors*, vol. 24, no. 12, Jun. 2024, doi: 10.3390/s24123911.
- [38] M. Farasat, D. Thalakatuna, Y. Yang, Z. Hu, and K. Esselle, "Suppression of common-mode resonance in multiband base station antennas," *Sensors*, vol. 23, no. 6, Mar. 2023, doi: 10.3390/s23062905.
- [39] C. Im, T. H. Lim, and H. Choo, "Design of a mmWave antenna printed on a thick vehicle-glass substrate using a linearly arrayed patch director and a grid-slotted patch reflector for high-gain characteristics," *Sensors*, vol. 22, no. 16, 2022, doi: 10.3390/s22166187.
- [40] M. Odiameni, H. J. Basherlou, C. H. See, N. O. Parchin, K. Goh, and H. Yu, "Advancements and challenges in antenna design and rectifying circuits for radio frequency energy harvesting," *Sensors*, vol. 24, no. 21, Oct. 2024, doi: 10.3390/s24216804.
- [41] T. D. Ha, X. Nie, H. Bağcı, D. Erricolo, and P.-Y. Chen, "A low-profile, wide-angle, and bandwidth-enhanced rectenna for radiative energy harvesting in the 12 GHz band," *IEEE Antennas and Wireless Propagation Letters*, vol. 23, no. 11, pp. 3807–3811, Nov. 2024, doi: 10.1109/LAWP.2024.3387925.
- [42] S. Abdollahi, A. Bakhtafrouz, and M. Maddahali, "Design of a beamforming tri-band rectifier for RF energy harvesting," *IEEE Access*, vol. 13, pp. 34802–34811, 2025, doi: 10.1109/ACCESS.2025.3544146.
- [43] J. Sang, L. Qian, M. Li, J. Wang, and Z. Zhu, "A wideband and high-gain circularly polarized antenna array for radio-frequency energy harvesting applications," *IEEE Transactions on Antennas and Propagation*, vol. 71, no. 6, pp. 4874–4887, Jun. 2023, doi: 10.1109/TAP.2023.3271526.
- [44] J. Ye and H. Gharavi, "Deep reinforcement learning-assisted energy harvesting wireless networks," *IEEE Transactions on Green Communications and Networking*, vol. 5, no. 2, pp. 990–1002, Jun. 2021, doi: 10.1109/TGCN.2020.3045075.
- [45] M. Joshi, K. Hu, C. A. Lynch, and M. M. Tentzeris, "Toward 5G wireless power harvesting: a promising broadbeam equiconvex lens-integrated mmWave harvester for smart city environments," *IEEE Microwave and Wireless Technology Letters*, vol. 35, no. 6, pp. 904–907, Jun. 2025, doi: 10.1109/LMWT.2025.3570677.
- [46] M. Saha, T. Khan, P. P. Shome, F. A. Talukdar, and S. R. Rengarajan, "Multi-resonant high gain antenna using dual-slots for 5G millimeter-wave energy harvesting applications," in *2025 Third International Conference on Microwave, Antenna and Communication (MAC)*, Jun. 2025, pp. 1–4, doi: 10.1109/MAC64480.2025.11140213.
- [47] Y. Wu, Q. Yang, and K. S. Kwak, "Energy efficiency maximization for energy harvesting millimeter wave systems at high SNR," *IEEE Wireless Communications Letters*, vol. 6, no. 5, pp. 698–701, Oct. 2017, doi: 10.1109/LWC.2017.2734087.
- [48] A. Alqasir, "An energy-saving scheme with edge computing and energy harvesting in mmWaves backhauling HetNets," *IEEE Access*, vol. 11, pp. 29116–29127, 2023, doi: 10.1109/ACCESS.2023.3259728.
- [49] K. Tang *et al.*, "Joint resource allocation for maximizing energy efficiency in mmWave-based wireless-powered communication networks," *IEEE Transactions on Vehicular Technology*, vol. 73, no. 6, pp. 8514–8528, 2024, doi: 10.1109/TVT.2024.3361032.
- [50] L. Chen, B. Hu, G. Xu, and S. Chen, "Energy-efficient power allocation and splitting for mmWave beamspace MIMO-NOMA with SWIPT," *IEEE Sensors Journal*, vol. 21, no. 14, pp. 16381–16394, Jul. 2021, doi: 10.1109/JSEN.2021.3076517.

BIOGRAPHIES OF AUTHORS



Mrs. Shalini Mirlle Gajendra     is an assistant professor in the Electronics and Communication Engineering, Dayananda Sagar Academy of Technology and Management, Bangalore, India. She is pursuing Ph.D. as a research scholar in BGS Institute of Technology, Adichunchanagiri University, B G Nagara, India, in the area of design of antennas for energy harvesting applications. She is a member of various profession bodies like IEEE, ISTE, IETE. She can be contacted at email: shalinimg.39@gmail.com.



Dr. Naveen Kalenahalli Bhoganna     is professor in Electronics and Communication Engineering, BGS Institute of Technology, Adichunchanagiri University, B G Nagara, India. He received his Ph.D. from VTU with a specialisation in VLSI Design and Embedded Systems. His research areas are VLSI, embedded systems, image processing, communication, and networking. He is a member of various profession bodies like IEEE, IEAE(InSc), ISTE, ISC and IET. During the last five years tenure at BGS Institute of Technology he was leading the targeted interventions, counselling and testing, information, education and communication, mainstreaming, surveillance divisions and various projects being implemented as a part of KSCST and other agencies. He has published more than 50 papers published in various conference and journals. He can be contacted at email: naveenkb@bgsit.ac.in.